Photonic band gap airbridge microcavity resonances in GaAs/Al_xO_y waveguides

D. J. Ripin,[a] Kuo-Yi Lim, G. S. Petrich, Pierre R. Villeneuve, Shanhui Fan, E. R. Thoen, J. D. Joannopoulos, E. P. Ippen, and L. A. Kolodziejski
Department of Physics, Department of Electrical Engineering and Computer Science, Research Laboratory of Electronics, Center for Material Science and Engineering, Massachusetts Institute of Technology, Cambridge, Massachusetts 02139-4307

(Received 1 April 1999; accepted for publication 27 October 1999)

Photonic band gap waveguide microcavities were designed, fabricated, and measured in a high-dielectric-contrast GaAs/Al_xO_y III–V compound semiconductor structure. The photonic crystal is defined by a regularly spaced one-dimensional array of holes in the waveguide. By controlling the spacing between the two central holes, the microcavity is formed. The waveguide microcavity is suspended in the airbridge geometry to further increase optical confinement. Resonance states with cavity quality factors as high as 360 were measured at wavelengths near 1.55 μm, with modal volumes as small as 0.026 μm^3. © *2000 American Institute of Physics.* [S0021-8979(00)06203-4]

Photonic band gap (PBG) crystals are being designed to control the emission and propagation of light, and for efficient electro-optic and telecommunication devices. A photonic crystal is a material with a spatially periodic dielectric constant.[1,2] Whereas light in optical fibers and waveguides is typically confined by total internal reflection, light in PBG crystals is controlled by Bragg reflection. A photonic crystal is said to have a PBG over a range of wavelengths if light over that wavelength range is Bragg reflected for all wave vector directions. This is analogous to the electronic energy band gap for a range of electron wave vectors in an electronic solid.

Resonant cavities can be created in a PBG crystal by the introduction of a local defect in the periodic refractive index lattice.[3] A defect can be a local deviation of either the periodicity or dielectric constant from a perfect lattice. The density of optical states will be modified and quantized by such a cavity. Typical semiconductor optical cavities, with dimensions greater than a cubic wavelength, have many resonant cavity modes within an atomic emission line shape. However a microcavity, confined in three dimensions to physical dimensions on the order of a few cubic half wavelengths, can have one or no modes overlapping an emission line. If there are no overlapping modes, the spontaneous emission of an atom in the cavity will be dramatically suppressed, while overlapping cavity and emission modes can enhance spontaneous emission.[4] In particular, the spontaneous emission can be enhanced relative to free space by the factor[5]

$$\eta = \frac{Q}{4\pi V_m}\left(\frac{\lambda}{n}\right)^3,$$

where λ is the mode wavelength in vacuum, Q is the quality factor defined by the number of cycles required for the cavity energy to decay by $e^{-2\pi}$, n is the cavity index of refraction, and V_m is the cavity modal volume.

Optical transmission measurements of a one-dimensional PBG air-bridge optical microcavity are presented here. A schematic of a typical device is shown in Fig. 1. Regularly spaced holes in a high-dielectric-contrast waveguide system lead to the formation of a one-dimensional PBG. A change in the spacing between the two center holes creates a microcavity with a resonant defect state inside the photonic band gap. Only one resonance state exists within the $>$300 nm wide PBG. The microcavity resonance peak was designed to be near the 1.55 μm optical communications wavelength. The GaAs/Al_xO_y III–V compound semiconductor material system allows future integration of active semiconductor structures within the microcavity. The waveguide containing the photonic crystal is suspended in air in the vicinity of the cavity to increase optical confinement and to suppress coupling to radiation from the cavity and substrate modes.[6] Monorail geometry devices, with an oxide layer remaining intact under the hole arrays, have been studied previously in the GaAs/Al_xO_y material system[7] and with Si/SiO_2.[8] Airbridge devices are expected to have higher Q's for than monorail devices for a given modal volume because of their increased confinement. One-dimensional PBG waveguide microcavities have also been studied in other geometries.[9,10]

Optical waveguiding and two-dimensional transverse confinement is generated by a high-dielectric-contrast waveguide system consisting of a GaAs ($n=3.37$) ridge waveguide layer on 3 μm thick Al_xO_y ($n=1.61$) to isolate the waveguide from the underlying GaAs substrate. The refractive index of the Al_xO_y was determined from transmission measurements of GaAs/Al_xO_y distributed Bragg reflectors. The measured waveguides are designed to be 214 nm thick and 593 nm wide, and therefore support only a single TE-like mode (electric field primarily parallel to the substrate at the center of the waveguide) in the wavelength range of in-

[a]Author to whom correspondence should be addressed; electronic mail: djripin@mit.edu

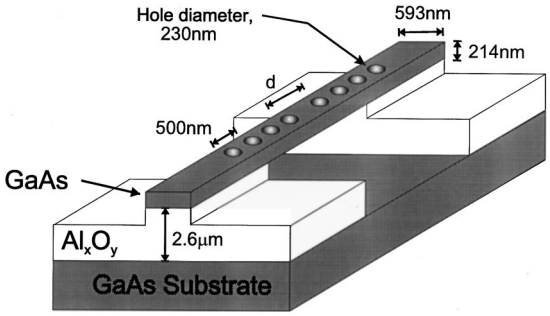

FIG. 1. Schematic of the photonic band gap airbridge microcavity. The waveguide extends 0.5 mm on both sides of the lattice of holes to allow for input and output coupling of light. The defect length *d* varies from waveguide to waveguide.

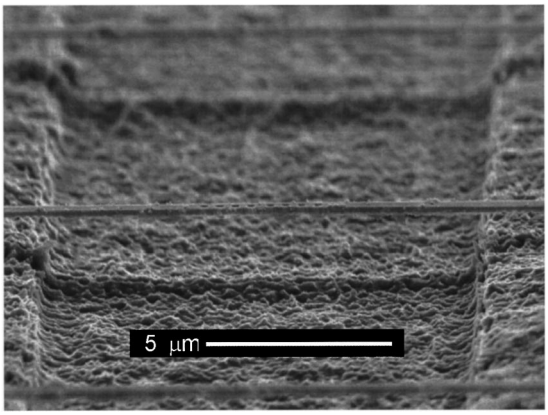

FIG. 2. Scanning electron micrograph (SEM) of a typical PBG airbridge device. Three waveguides are shown running from left to right; the center waveguide is in focus, and the waveguides in the foreground and background are out of focus. The waveguides are suspended over a 10 μm wide trench of Al_xO_y material. In the middle of the center waveguide eight holes form the photonic crystal lattice. The center-to-center separation between the middle two holes is different from sample to sample to form a microcavities with different resonance wavelengths.

terest. The waveguides extend 0.5 mm on both sides of the suspended airbridge for efficient coupling into and out of the microcavity, and the waveguide's width is flared to 2 μm at the input facet to improve coupling of light into the waveguides. Eight holes are defined to be 230 nm in diameter, and are separated by 500 nm center to center. The separation between the two center holes determines the wavelength of the resonant cavity mode, and has been varied from device to device. Subject to the fabrication constraints, devices were designed to have small modal volumes while maintaining high peak transmission. These constraints set a limit on the *Q* of the device.

The first fabrication step for the airbridge structures is the growth of a $GaAs/Al_{0.93}Ga_{0.07}As$ heterostructure on a GaAs substrate using gas source molecular beam epitaxy.[10,11] A 100 nm thick layer of silicon dioxide (SiO_2) is then deposited onto the surface using plasma-enhanced chemical vapor deposition, followed by spinning on a 200 nm thick layer of polymethylmethacrylate (PMMA). The waveguide and photonic crystal structures are defined in the PMMA using direct-write electron beam lithography. After developing the PMMA, a 30 nm layer of nickel (Ni) is deposited by electron-beam evaporation. Following a lift-off process, only the Ni film over the electron-beam-written pattern remains, and serves as a mask for the device pattern. The pattern in the Ni is then transferred into the SiO_2 by a reactive ion etch (RIE) process. After the Ni is removed λ_r with an acid etch, the SiO_2 is used as a mask for the RIE of the GaAs layer using $BCl_3/SiCl_4$.

Next, optical lithography is used to define a 10 μm wide trench area underneath the photonic crystal. A RIE step is used to create a trench about 800 nm deep into the $Al_{0.93}Ga_{0.07}As$ layer. The photoresist and SiO_2 layers are removed by RIE processes. The $Al_{0.93}Ga_{0.07}As$ layer is converted to Al_xO_y by oxidation at 435 °C for 30 min using steam in N_2 carrier gas. Optical lithography is used again to redefine the airbridge suspension trench. Finally, the waveguide is suspended by the sacrificial etch of Al_xO_y using a diluted hydroflouric acid solution. A scanning electron micrograph (SEM) of a suspended airbridge microcavity is shown in Fig. 2.

Theoretical optical transmission spectra have been computed using a finite-difference time-domain algorithm.[12,13] A typical computed spectrum is shown in Fig. 3. Transmission is close to zero in the PBG region from 1400 to 1700 nm. The microcavity resonance has a Lorentzian line shape centered at 1550 nm, and has a computed *Q* of 320. Transmission at the maximum of the resonance peak is 94% of the input intensity. The transmission is limited by coupling of the cavity mode to radiation modes.

Transmission spectra of the devices are studied using the continuous wave output of a $NaCl:OH^-$ laser. The laser source provides a tuning range from 1500 to 1680 nm, with a power of ~250 mW at the gain peak, and a linewidth of approximately 0.1 nm. The laser light is coupled into a fiber, of which 3% is coupled to a power detector to monitor the laser power. The remaining light is coupled into the waveguide devices through a fiber–lens assembly. Polarization was controlled with a polarizing beam splitter cube, a half-

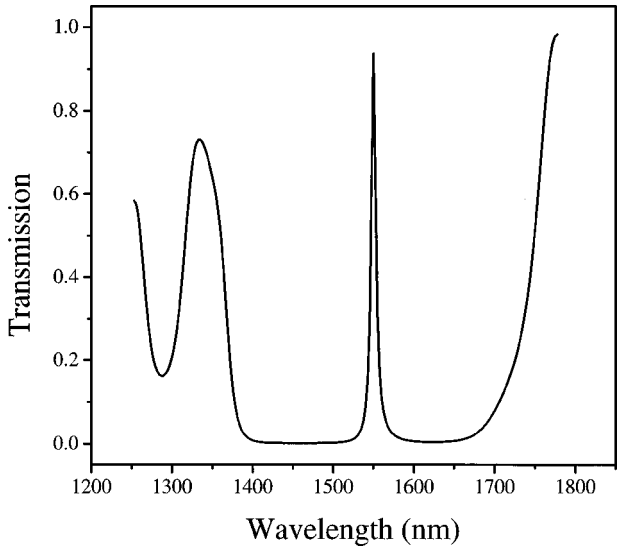

FIG. 3. Theoretical transmission through a PBG airbridge microcavity. At the resonance wavelength, a maximum of 94% of the input intensity is transmitted. The theoretical cavity *Q* is 320.

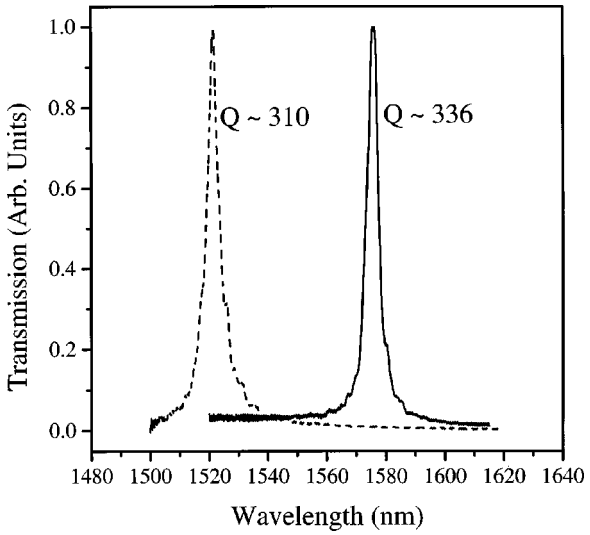

FIG. 4. Transmission spectrum measured through two different PBG airbridge microcavities. The long and short wavelength resonances have defect center-to-center lengths of 632 and 703 nm, respectively. The maximum of the resonance peaks are normalized to unity.

wave plate, and a quarter-wave plate before the fiber–lens assembly. All measurements are taken with TE polarization, as TM light was not guided. The output of the waveguide is imaged with either a microscope objective or an aspheric lens through a 100 μm pinhole in order to suppress substrate guided light. A photodetector is placed after the pinhole to monitor the output power, and the wavelength is recorded using an optical spectrum analyzer.

Losses of 3–6 dB/mm have been measured through straight waveguides without a photonic crystal device, by imaging the top of the waveguide with an infrared camera. The intensity of the light scattered out of the waveguide as a function of position can be used to estimate the linear loss. As expected, scattering from sidewall and GaAs/Al_xO_y interface roughness, and *e*-beam lithography field stitching errors appear to be the dominant loss mechanisms, and are a accentuated by the tight optical confinement in the high-dielectric-contrast waveguide system. At high input powers, two photon absorption has been observed. Based on the estimated loss, waveguide input coupling efficiencies of ~3% were calculated.

Figure 4 shows the normalized experimental transmission through two distinct airbridge microcavities, having defect sizes of 632 and 703 nm, respectively from hole center to center. The resonance states that are shown have Q's of 310 and 336, respectively; resonance Q's as high as 360 have been recorded. The measured Q's are calculated by the relation $Q=\lambda/\Delta\lambda$, where $\Delta\lambda$ is the full-width-at-half-maximum of the resonance peak, and λ_r is the resonance's center wavelength. As expected, the resonance shifts to longer wavelengths as the microcavity size is increased. Because the PBG is calculated to be over 300 nm wide, the band edges are not visible within the 180 nm tuning range of the laser. Due to the lack of a precise loss measurement or a band edge within the experimental window, the maxima of the peaks in Fig. 4 are normalized to unity rather than to absolute transmission. The devices have a modal volume of 0.046 μm^3 given by

$$V_m=\frac{\int \varepsilon \mathbf{E}^*\cdot\mathbf{E}\, d^3\mathbf{r}}{(\varepsilon \mathbf{E}^*\cdot\mathbf{E})_{\max}},$$

where $\mathbf{E}$ is the electric field, ε is the dielectric constant of the cavity material, and $(\varepsilon\mathbf{E}^*\cdot\mathbf{E})_{\max}$ is the maximum power in the electric field in the cavity. The modal volume, computed using a three-dimensional vector finite-difference time-domain method, is only $2(\lambda/2n)^3$. Using the modal volume, Q, and a peak wavelength from one sample, a maximum enhancement factor for spontaneous emission is computed to be $\eta=72$.

By scaling the dimensions of the photonic crystal, a photonic band edge was observed within the laser tuning range. One device showed a band edge at 1620 nm, with ~30 dB attenuation for light inside the band gap compared to outside the PBG. In another scaled device, both a band edge and the resonance were observed in the laser tuning window. With the top of the band edge normalized to 100%, a maximum absolute transmission of 72% was determined on resonance at 1512 nm, with a Q of 230. The Q is lower because the resonance is shifted closer to the band edge, where it will experience higher coupling to continuum states.[9]

Resonant microcavities with modal volumes around 0.026 μm^3 have been designed, fabricated, and measured in one-dimensional photonic band gap airbridge structures. Cavity quality factors as high as 360 in the were measured 1.55 μm regime. Furthermore, the airbridges have been fabricated in the GaAs/Al_xO_y III–V compound semiconductor system, which can be used to integrate active semiconductor devices with PBG optical microcavities. The high dielectric contrast GaAs/Al_xO_y system could be used for nanoscale optoelectronic device integration or as the basis of a low-threshold laser system with fast modulation.

The authors would like to thank Dr. Günter Steinmeyer for his assistance in planning the experiment. This work was supported in part by the MRSEC program of the NSF under Award No. DMR-9400334.

[1] E. Yablonovitch, Phys. Rev. Lett. **58**, 2059 (1987).
[2] J. D. Joannopoulos, P. R. Villeneuve, and S. Fan, Nature (London) **386**, 143 (1997).
[3] J. D. Joannopoulos, R. D. Meade, and J. N. Winn, *Photonic Crystals* (Princeton University Press, Princeton, NJ, 1995).
[4] D. Kleppner, Phys. Rev. Lett. **47**, 233 (1981).
[5] H. Yokoyama and S. D. Brorson, J. Appl. Phys. **66**, 4801 (1989).
[6] P. R. Villeneuve, S. Fan, J. D. Joannapoulos, K.-Y. Lim, G. S. Petrich, L. A. Kolodziejski, and R. Reif, Appl. Phys. Lett. **67**, 167 (1995).
[7] K.-Y. Lim *et al.*, J. Vac. Sci. Technol. B **17**, 1171 (1999).
[8] J. S. Foresi *et al.*, Nature (London) **390**, 143 (1997).
[9] T. F. Krauss, B. Vögele, C. R. Stanley, and R. M. De La Ru, IEEE Photonics Technol. Lett. **9**, 176 (1997).
[10] J. P. Zhang, D. Y. Chu, S. L. Wu, W. G. Bi, R. C. Tiberio, R. M. Joseph, A. Taflove, C. W. Tu, and S. T. Ho, IEEE Photonics Technol. Lett. **8**, 491 (1996).
[11] K.-Y. Lim, D. J. Ripin, G. S. Petrich, P. R. Villeneuve, S. Fan, J. D. Joannopoulos, E. P. Ippen, and L. A. Kolodziejski, Adv. Mater **11**, 501 (1999).
[12] P. R. Villeneuve, S. Fan, S. G. Johnson, and J. D. Joannopoulos, IEE Proc. Optoelectron. **145**, (1998).
[13] K. S. Kunz and R. J. Luebbers, *The Finite-Difference Time-domain Method for Electromagnetics* (CRC, Boca Raton, 1993).